Investigations of the Reactions Involved in Formation of the Light-Sensitive Phases in Thermally Developed Photomaterials

Yu. E. Usanov and T. B. Kolesova

S. I. Vavilov State Optical Institute, Birzhevaya Line, 12, 199034 St. Petersburg, Russia

We have carried out electrochemical, sensitometric, and electron microscope investigations of the reactions of the photosensitive phase of a thermally developable photomaterial. We have found that formation of microcrystals of silver bromide by metathetical reaction of silver stearate with bromide in aqueous solution leads to precipitation of silver bromide as a separate phase, accompanied by dissolution of silver stearate microcrystals. The size of the AgBr microcrystals increases with increasing concentration of the brominating agent, but does not exceed 0.07 μm. Latent image centers formed by the AgBr microcrystals are capable of catalyzing thermal development if the microcrystals have been formed in the presence of the carboxylate. The process of thermal amplification of the latent image centers may, however, be achieved on AgBr crystals having no physical contact with silver stearate. We propose that thermal development of latent image centers on AgBr crystals proceeds by diffusion of silver stearate-derived "droplets" to the development centers. Fog formation, on the other hand, nucleates independently of the AgBr microcrystals.

Journal of Imaging Science and Technology 40: 104 – 110 (1996)

Introduction

Thermally developing photomaterials (TDPMs) based on silver halides and silver carboxylates are widely used in optical imaging systems. The light-sensitive phase of the TDPM is silver halide (AgHal), which can be chemically and optically sensitized. The developing agent may be incorporated in either the photosensitive layer or a protective layer. Development of the exposed TDPM is carried out by heating the film to 110–130°C for no more than 10–20 s.[1,2] It has been suggested that, as result of the decrease of polymer binder viscosity[1] or phase transition in the silver carboxylate,[2] under these conditions the silver carboxylate dissociates and silver ions are reduced on the latent image centers by the developer. From the former perspective it can be understood that the TDPM film should not contain gelatin, which in the dry state does not melt upon heating. Thermally processed photomaterials using gelatin binder have been described, but these materials require addition of thermal solvents[3a] or a small amount of water[3b] to enable diffusion of the reagents on heating. Cessation of heating causes the diffusion processes in the TDPM layer to decelerate.

The simplest method of forming the light-sensitive phase in TDPM is to add bromide to a polymer solution containing a dispersion of silver carboxylates. TDPMs made by this method have low sensitivity, corresponding to 0.1–0.01 ISO. This sensitivity level suggests that microcrystals (MC) of AgHal may have the same dimensions as in holographic emulsions, i.e., 100–300 Å.[4] More recent TEM investigations have suggested dimensions of the order of 60 Å.[2,5] We infer that the sensitization and MC growth processes in a polymer are not as effective as in a gelatin solution.

The goal of the present work is to investigate the reactions that occur during the formation of the light-sensitive phase in Ag carboxylate–AgHal systems. To this end we used a potentiometric titration method. We also investigated the sensitometric properties of TDPM samples having different silver halide to silver stearate (AgSt) ratios. These results were further compared with the transmission electron microscopy (TEM) results obtained on photolayer cross sections.

Experimental

The potentiometric titration method employed glass and silver electrodes to measure pH and E_{Ag} (mV versus standard calomel electrode) changes in solution in the course of the reactions carried out as described later. All solutions were prepared in distilled water.

Silver carboxylate samples were prepared with various concentrations of silver bromide. All reagents were of the purest available grades. Samples were prepared as follows: Into a reactor with a stirrer, containing 250 mL of distilled water and 0.02 mol melted stearic acid at 82°C, 30 mL each of aqueous solutions of 0.475 M NaOH and 0.495 M $AgNO_3$ were introduced sequentially, dropwise with stirring, over 5-min periods. The resulting suspension of silver stearate was cooled to 28°C, and, with intensive mixing, a separate amount of 1.0 M solution of LiBr was added under a safelight. Ripening time was 30 min. Then the precipitate was poured at room temperature onto a paper filter in a Büchner funnel and washed with distilled water until a test for the presence of silver ions in the wash water was negative. In the discussion to follow the ratio of AgBr to AgSt is designated "at synthesis."

The silver salt precipitate was dried with isopropanol and then placed into a ball mill containing 50 mL of 7.5% polyvinylbutyral (PVB) and 0.8% phthalimide in isopropanol. Dispersion of the silver salt in PVB was thus carried out for 3 h at room temperature. Dispersions of silver stearate in PVB were accordingly obtained with different degrees of bromination. These dispersions were subsequently mixed in specific proportions with similar suspensions of bromide-free AgSt to prepare the final thermally developable composition (TDC). The AgBr to AgSt ratios obtained at this point are designated "in TDC."

Original manuscript received August 22, 1995. Revised January 24, 1996.

For preparation of the TDPM, succinimide, a merocyanine dye, and a developing agent, 2,2'-methylene-*bis*-(4-methyl-6-*tert*-butylphenol), were added sequentially to 10 mL silver salt suspension in PVB over 5-min intervals. Optimal quantities of these substances in the TDC had been determined in earlier work at the S. I. Vavilov State Optical Institute in the 1986–1988 time frame. The suspension of the TDC was coated on polyester film and dried. The thickness of the dry photolayer was 8–10 μm, which corresponds to a silver coating weight of ca. 1.5 g total Ag/m^2.

Samples of TDPM were exposed for 30 s through a step tablet (0.15 optical density increments) to white light on an FSR-41 sensitometer and developed for different times on a heated, thermally stabilized drum at 115°C. To determine light sensitivity of the AgBr in the TDC without thermal amplification, similarly exposed samples were tray-developed at room temperature, with agitation, in freshly prepared aliquots of a solution having the following composition:

Metol (*p*-methylaminophenol sulfate)	3.0	g
Hydroquinone	3.0	g
Anhydrous sodium sulfite	40.0	g
Sodium carbonate	10.0	g
Potassium bromide	5.0	g
Isopropanol	300	mL
Water to	1	L

Development time in this solution was 2.5 min at 20°C.

Optical densities of the step tablet images obtained with either thermal or wet development were measured with a DP-1 transmission densitometer. Results were used to construct characteristic curves and to determine the sensitometric parameters of TDPM samples: sensitivity, $S_{0.2}$ (measured at a density of 0.2 over fog), contrast coefficient (γ), optical density of fog (D_o), and maximum density (D_{max}). For TEM investigations, 130-nm-thick cross sections of films embedded in epoxy resin, obtained using an ultramicrotome, were imaged in a JEM-7 electron microscope. The accelerating voltage was 80 kV. Prints with magnifications from 16,000× to 60,000× were prepared. Representative TEM images are shown later in Figs. 4 and 5. In all cases images are magnified, cropped, and presented so that the full horizontal width of the frame corresponds to 1.5 μm on the sample.

Results and Discussion

Electrochemical Measurements. Formation of the alkali metal stearate proceeds according to the reaction

$$HSt + NaOH \longrightarrow NaSt + H_2O. \quad (1)$$

Precipitation of silver stearate then occurs according to the reaction

$$NaSt + AgNO_3 \longrightarrow AgSt + NaNO_3. \quad (2)$$

Changes in pH and in E_{Ag} in the course of this reaction, observed on titrating 250 mL aqueous 0.0142 M NaOH in the presence of 0.006 M stearic acid at 82°C with a 1.0 M solution of $AgNO_3$ are shown in Fig. 1(a), Curves 1 and 2, respectively. Curve 5 in Fig. 1(a) characterizes the change of E_{Ag} when 1 M $AgNO_3$ solution was added into a melt of HSt in water at 82°C.

Bromination of silver stearate in water proceeds according to the metathetical reaction:[2,4–6]

$$AgSt + LiBr \longrightarrow AgBr + LiSt. \quad (3)$$

The byproduct, LiSt, is water-soluble. Both pH and E_{Ag} were measured during the titration of 0.0142 mol silver stearate dispersed in 250 mL of water in the presence of 0.006 M stearic acid with 1 M LiBr at 28°C, as shown in Fig. 1(b), Curves 3 and 4, respectively.

Analysis of the titration curves shows from the initial condition of Curve 1, Fig. 1(a), that Reaction 1 between the weak acid and strong alkali results in the formation of the salt at pH = 9.8 in solution. During Reaction 2 the

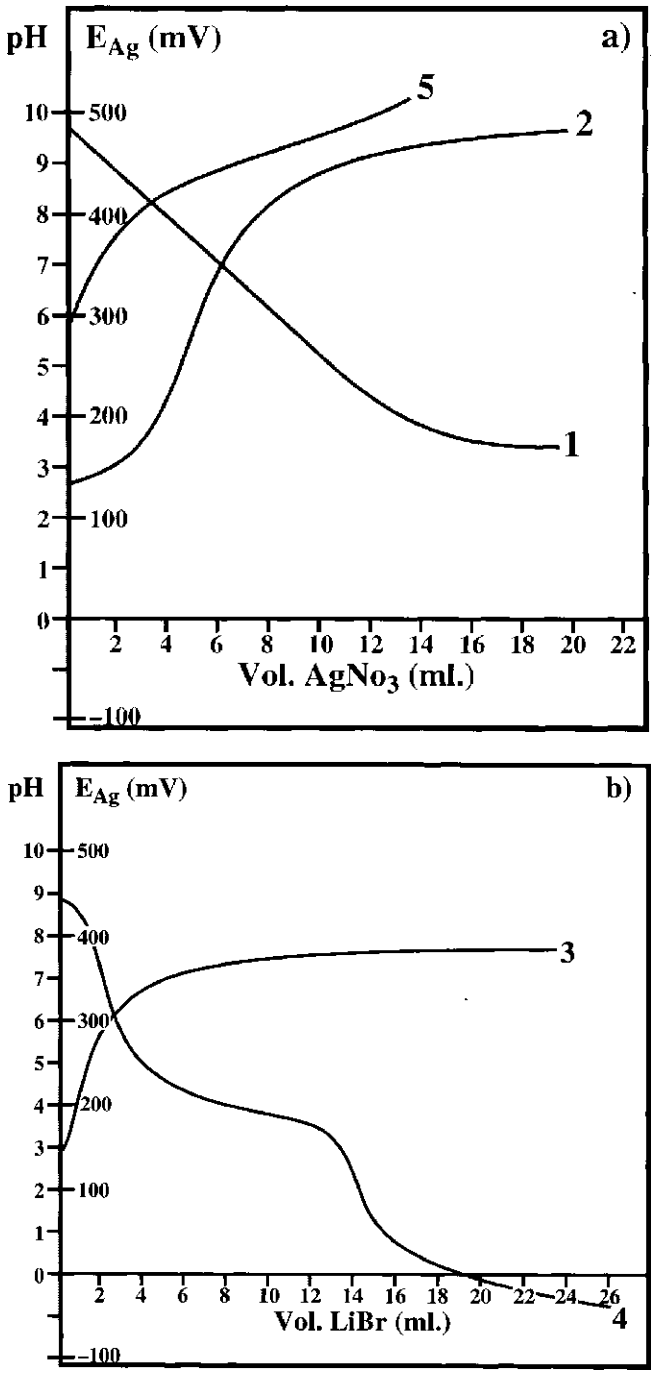

Figure 1. Values of pH and E_{Ag} in the course of the titration processes: (a) Curves 1 and 2 correspond to pH and E_{Ag}, respectively, of an aqueous solution of NaSt titrated with $AgNO_3$ solution at 82°C; and Curve 5 represents E_{Ag} of a melt of HSt dispersed in water titrated with $AgNO_3$ solution. (b) Aqueous suspension of silver stearate titrated with LiBr solution; Curves 3 and 4 correspond to pH and E_{Ag}, respectively.

pH of the solution decreases (Curve 1); from E_{Ag} (Curve 2) we infer that an excess of silver ions is present in solution beyond the equivalence point. Introduction of $AgNO_3$ solution into a stearic acid melt [Fig. 1(a), Curve 5] results in observable turbidity of the melt along with a higher silver electrode potential, compared with that corresponding to the same silver ion concentration in the presence of NaSt, which is indicative of an incomplete reaction between $AgNO_3$ and HSt under these conditions.

Curves 3 and 4 of Fig. 1(b), illustrating the silver stearate bromination process, are the most interesting: Curve 4 shows the relationship $pAg = f(C_{LiBr})$, which has a segment almost parallel to the abscissa. This curve shows that increasing the bromide concentration does not change the potential of the silver electrode in this regime, although the pH of the solution continues to increase slightly (Curve 3). Based on Curves 3 and 4, we infer that with $E_{Ag} < 210$ mV the surface of the stearate MC is saturated with bromide. Subsequent addition of LiBr results in stearate bromination internally within the MC. Thus a constant value of E_{Ag} is observed, which is determined only by the dissociation of the silver salt on the surface of the MC. The pH increase (Curve 3) indicates, however, that dissolution of stearate anion continues to take place on addition of bromide.

Sensitometry. Figure 2 shows typical characteristic curves obtained for TDPM samples with high [0.40:1; Fig. 2(a)] and low [0.06:1; Fig. 2(b)] ratios of AgBr:AgSt. Comparison of the curves shows that at high bromide content the highly exposed areas exhibit a decrease in the optical density as development time is increased. At the same time, optical density of fog constantly increases more or less in parallel with the optical densities corresponding to exposures on the linear portion of the characteristic curve. For the sample with low silver bromide content, optical densities for all exposure levels increase with increasing development time.

Table I summarizes the sensitometric parameters of TDPM samples developed at 115°C for 10 s. As can be seen from these data, sensitometric responses may not be optimal for all samples, but they allow the following inferences to be drawn. Where AgBr:AgSt in the TDC is ≤ 0.1:1, full development to $D_{max} \geq 1.5$ is impossible. We infer that this amount of AgBr is insufficient to sensitize all the silver carboxylate present in the TDPM. In the case of Samples 1.1 to 1.3, low speed indexes, $S_{0.2}$, may also be

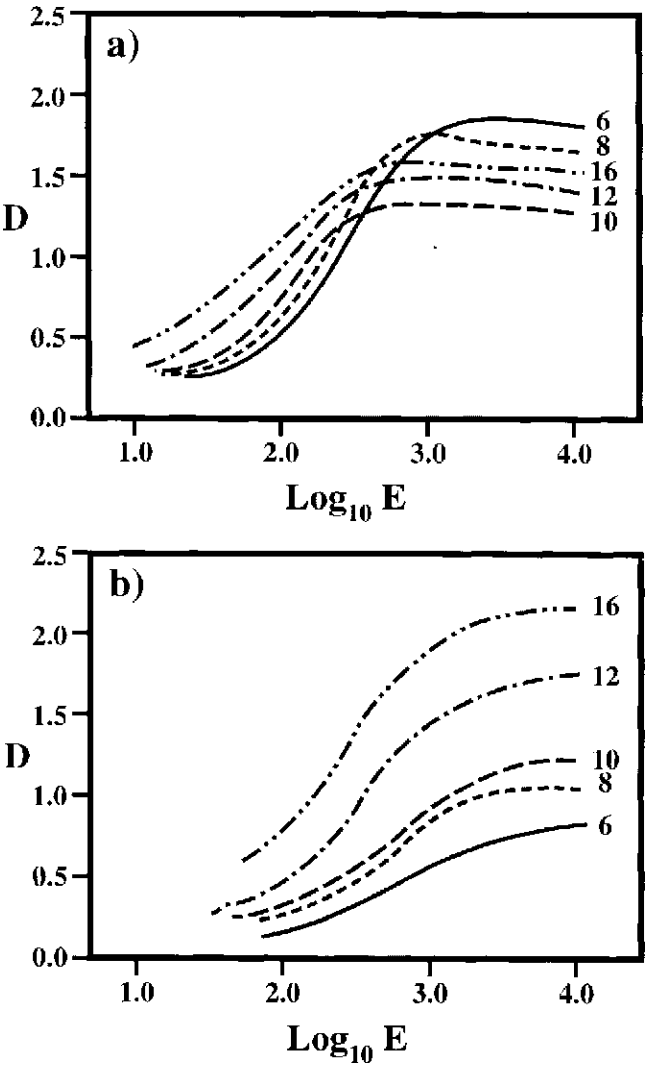

Figure 2. Characteristic curves of TDPM samples with AgBr:AgSt ratios of (a) 0.40:1 and (b) 0.06:1. Numbers on the curves indicate development times in seconds at 115°C.

TABLE I. Sensitometric Properties of Thermally Developed TDPM

Sample	Ratio AgBr:AgSt		Sensitometric parameters			
	At synthesis	In TDC	$S_{0.2}$	γ	D_o	D_{max}
1.1	0.11:1	0.03:1	0.2	0.3	0.10	0.30
1.2	0.11:1	0.05:1	0.9	0.5	0.15	0.70
1.3	0.11:1	0.08:1	1.5	0.8	0.15	0.90
2.1	0.25:1	0.06:1	10.0	0.7	0.18	1.29
2.2	0.25:1	0.11:1	11.0	1.2	0.21	2.06
2.3	0.25:1	0.16:1	12.0	1.2	0.21	1.71
2.4	0.25:1	0.25:1	14.0	1.4	0.19	1.77
3.1	0.67:1	0.14:1	12.0	1.4	0.22	1.91
3.2	0.67:1	0.25:1	15.0	1.4	0.22	1.68
3.3	0.67:1	0.40:1	18.0	1.3	0.19	1.52
3.4	0.67:1	0.66:1	22.0	1.4	0.19	1.29
4.1	2.01:1	0.07:1	4.5	0.9	0.13	1.34
4.2	2.01:1	0.25:1	12.0	1.3	0.20	1.74
4.3	2.01:1	0.51:1	18.0	1.9	0.28	1.92
5.1	Complete	0.25:1	25.0	2.1	0.23	2.29
5.2	Complete	Complete	1.0	0.2	0.51	0.71

TABLE II. Comparison of Sensitivity (as Number of Visually Discernible Steps Following Step Tablet Exposure) of TDPM on Thermal and Solution Development

Sample*	Number of visible steps developed	
	Thermally	Solution
1.1	8	6
1.2	9	7
1.3	11	8
2.1	15	12
2.2	16	13
2.3	17	14
2.4	17	15
3.1	18	15
3.2	18	15
3.3	20	17
3.4	19	16
4.1	14	12
4.2	17	14
4.3	16	14
5.1	16	14
5.2	13	15

* See Table I.

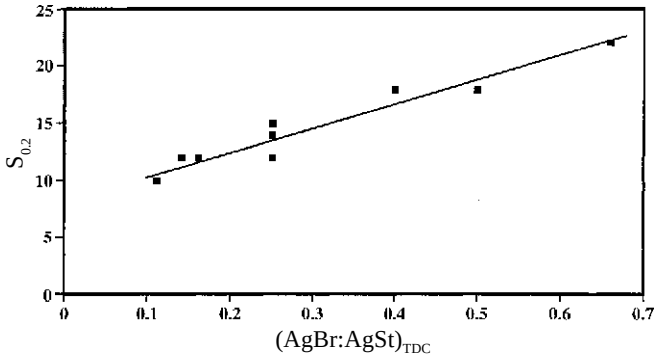

Figure 3. Scatter graph of photothermographic speed, $S_{0.2}$ (Table I), versus AgBr:AgSt level in coated TDPMs.

attributed to a very small size for the AgBr MCs when AgBr:AgSt = 0.11:1 at synthesis. Above this threshold, the sensitometric properties are dependent primarily on the amount of AgBr in the TDC, not on the degree of the initial silver stearate bromination at synthesis. Thus regression of $S_{0.2}$ on AgBr:AgSt in the TDC yields

$$S_{0.2} = 8.4 + 20.5\ (AgBr:AgSt)_{TDC} \quad (4)$$

with a correlation coefficient of $r = 0.967$. The scatter graph is shown in Fig. 3. Samples 5.1 and 5.2 do not fall on the line of Eq. 1; the high speed of Sample 5.1 suggests that the process of synthesis of AgBr by complete halidization of AgSt yields a uniquely sensitive TDC. An attempted regression analysis of $S_{0.2}$ on the ratio of AgBr:AgSt at synthesis yielded a statistically insignificant correlation coefficient of 0.426.

On the basis of these results, we hypothesize that the AgBr MCs reach a definite size and then stop growing even as the level of silver stearate bromination increases. This is consistent with the "sphere of influence" model of Klosterboer,[2] insofar as increasing AgBr content above a threshold level introduces more than one light-sensitive MC in each development domain, thus leading to redundancy in latent image formation.

Increasing the amount of AgBr in the TDC results in an increase of light sensitivity as shown in Fig. 3, owing to increased light absorption, but it also correlates with decreasing D_{max}, with $r = -0.936$; Sample 5.1 again does not fit the correlation. We attribute loss of D_{max} to formation of smaller Ag(0) particles during development. These particles have absorption maxima only in the short-wave range of the spectrum, similar in this respect to colloidal silver.[7] Formation of smaller silver particles on development may reflect redundancy of nucleation, i.e., of latent image sites, owing to redundancy of silver halide grains within a single sphere of influence.

Solution Development. The light sensitivity of TDPM samples processed in the developer solution, reported as number of steps, N, visually discernible in the developed image of the step tablet exposure, was compared with the sensitivity of samples of the same TDPMs, identically exposed, on thermal development. These data are presented in Table II. Thermal and wet development sensitivities parallel one another, but the number of visible steps is consistently higher for thermal development. Thus

$$N_{solution} = 0.93N_{thermal} - 1.5, \quad (5)$$

with $r = 0.991$. This difference in absolute number of discernible steps for the two modes of development is explained in part by the low optical density achieved when only the AgBr MCs are developed, as we believe to be the

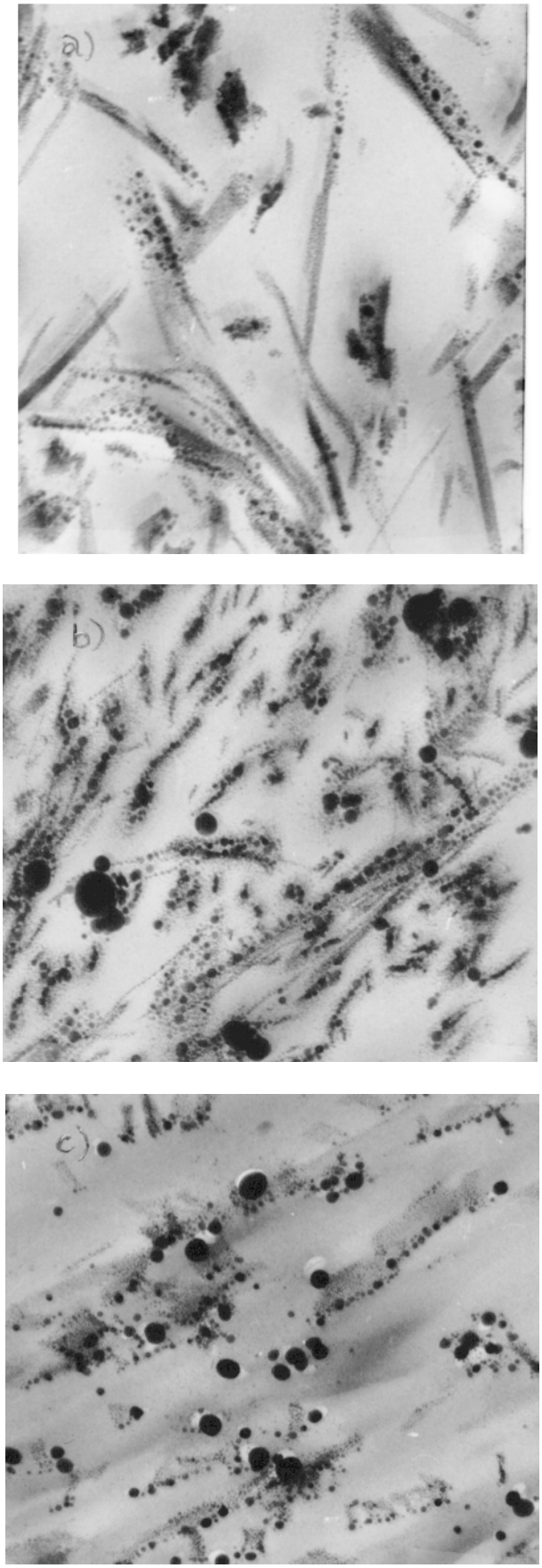

Figure 4. TEM images of (a) TDPM sample containing no AgBr, as coated; (b) after heating to 115°C; and (c) unheated sample of formulation 3.2 (Table I).

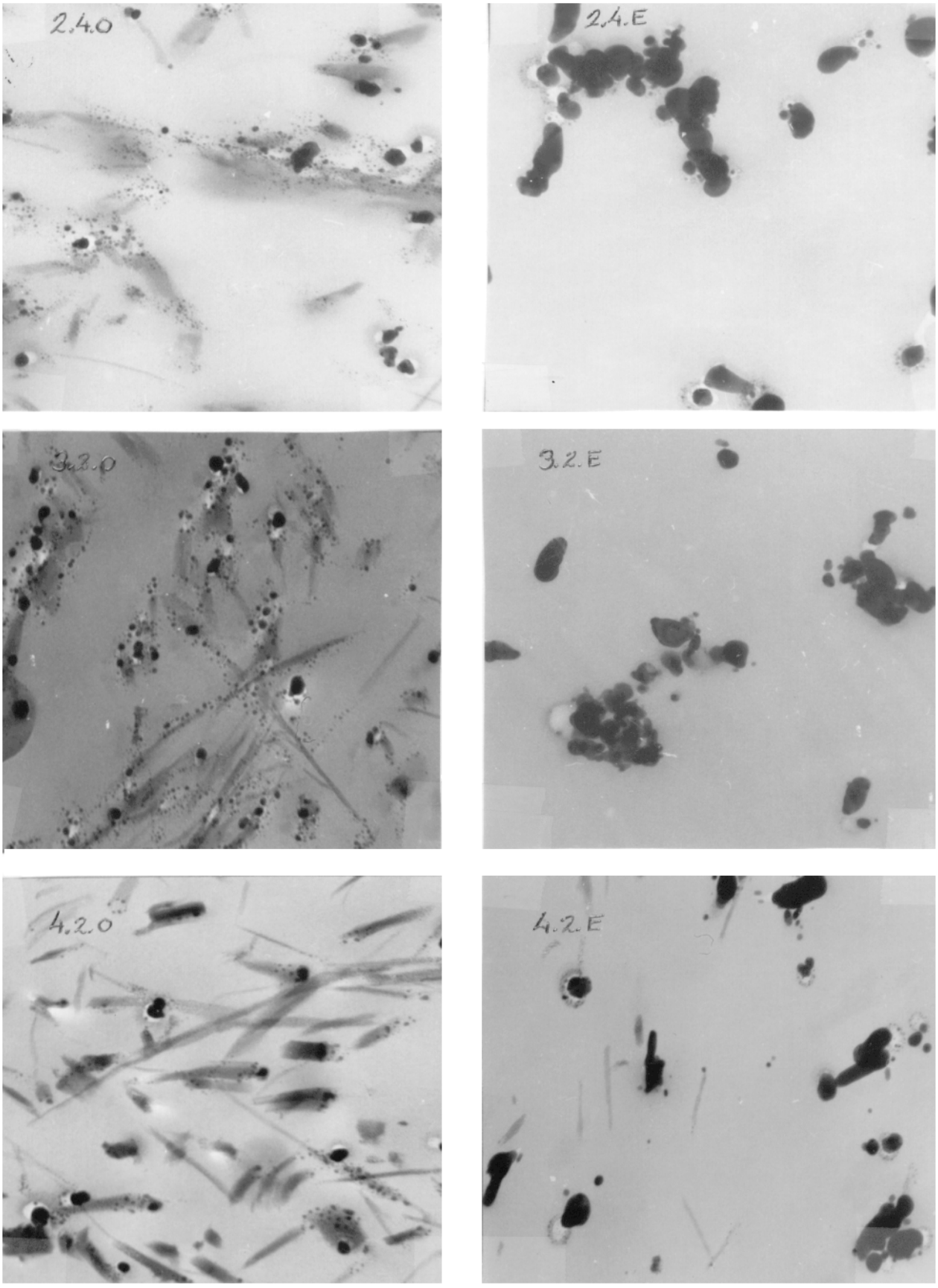

Figure 5. As Fig. 4 , but for TDPM incorporating AgBr; indexes on individual frames correspond to those in Table I: E indicates sample exposed and developed at 115°C for 10 s (image); O indicates unexposed, developed sample (fog).

case for solution development of the TDPMs. We interpret these results as showing that under our conditions the process of thermal amplification yields light sensitivity corresponding to that obtained by surface development of the same AgBr MCs, and we further speculate that thermal development corresponds to amplification of the surface latent image centers on the AgBr MCs.

It is of interest to note that Sample 5.2, which contains only AgBr MCs, is slower when developed thermally than when developed in solution. This result supports the hypothesis that thermal development reduces primarily silver ions from silver carboxylate and not from silver halide,[2,5] whereas the opposite is true for solution development.

TEM Investigations. To determine the influence of the extent of halidization on the structure of AgBr crystals and of the developed silver, TEM investigations of microsections of the TDPM films were performed. The general microstructure of the photolayer and the properties of some microcrystals of silver salts and developed particles could be observed. Figures 4 and 5 show examples of the TEM images of our TDPM samples. Fig. 4(a) shows an undeveloped layer containing silver stearate with all the additives introduced into the TDC, but without silver bromide; Fig. 4(b) shows the same material as in Fig. 4(a), but the layer has been thermally developed.

The samples shown in Fig. 5 were obtained with different AgBr:AgSt ratios during synthesis, but contain the same ratio of silver bromide and silver stearate (0.25:1) in the TDC. The pictures have designations corresponding to those in Table I. Additional labeling of samples indicates the following: "E" is exposed and developed at 115°C for 10 s to $D = (1.40 \pm 0.1)$; "O" is developed without exposure (fog).

By inspection and comparison of the micrographs presented in Figs. 4 and 5 we observe the following. Microcrystals of AgSt can be seen very clearly in Figs. 4(a), (b), and (c). On the surfaces of these MCs there is a distribution of fine spheroidal particles ranging in size from 0.05 μm to the limit of discernibility at 60,000× magnification, i.e., ca. 50 Å. Compared with silver stearate and binder, these spheroids are considerably more opaque to the transmission electron beam. This increased opacity indicates an increased concentration of silver ions. These particles are morphologically distinct from beam damage, which is observed in the present samples only on prolonged exposure to the 80 kV electron beam in the electron microscope. Their size distribution is clearly bimodal; the distance between droplets is comparable to their diameters. They are nonuniformly distributed on the surfaces of individual MCs, as well as among various crystals.

One possibility is that these spheroidal particles appear as a consequence of dissolution of the silver stearate and stearic acid present in the layer under conditions of synthesis of the MC and redispersion, especially in the presence of the complexing agent, succinimide. In this case, the redispersed composition exists in a phase that has an increased concentration of silver ions on the surface surrounding the spherical micelles.

Heating the film to 115°C [Fig. 4(b)] results in decomposition of AgSt into separate nanoparticles whose spatial distribution replicates the shape of the original AgSt MC. Further heating results in coagulation of these fine particles into larger ones, consistent with the thermodynamics of phase formation.[8] Comparison of Fig. 4(a) with 4(c), which shows an unprocessed sample of AgBr containing formulation 3.2, indicates that the brominated photolayer contains compact particles, opaque to the electron beam, which assign as AgBr MCs. Their distinguishing features relative to the spheroids seen in Fig. 4(a), as well as in Fig. 4(c), are not only their significantly larger sizes, but also the surrounding halos, which are more transparent to the electron beam than are either the silver stearate or the binder.

These halos may be the result of the metathetical reaction to produce silver bromide from silver stearate, i.e., local depletion of the stearate phase in silver ion. In this case, they indicate that AgSt remains only in the outer sphere, relative to AgBr. The majority of the MCs of AgBr formed by metathetical reaction are thus separated from the MCs of silver stearate. Representative histograms of their particle size distributions are shown in Fig. 6.

Frames 2.4.E, 3.2.E, and 4.2.E in Fig. 5 show silver particles formed in the exposed photolayers upon thermal development to D = ca. 1.4. All three formulations are characterized by a constant ratio, AgBr:AgSt = 0.25:1. In Sample 4.2.E, initially synthesized with the highest bromide concentration, the silver stearate is not completely reduced, even though it exhibits the same optical density as samples formulated at lower bromide levels (2.4.E. and 3.2.E), which suggests that in Sample 4.2.E the developed silver particles have either uniquely high covering power or high concentration. In the samples with lower initial AgBr:AgSt ratios, residual silver stearate was not observed. Residual AgSt in developed sample 4.2E does not show a significant population of the droplets observed in unprocessed samples. We infer that they have been consumed in the thermal amplification process.

The developed, exposed photolayers show transparent halos around a number of the particles identified as silver(0), similar to those observed in connection with formation of the AgBr MCs (above). Sometimes halos have elongated shapes in the form of streaks connecting developed particles, or in the form of transparent traces from the particle and into the surrounding polymer. These streaks are observed only in developed samples of TDPM.

The silver deposit in the exposed and developed photolayers comprises aggregates of smaller sized spheroidal particles, and in a number of cases the streaks left by these particles during apparent diffusion toward the centers of aggregation are evident. Continued aggregation of spheroidal silver particles can lead to decreased covering power, i.e., decreased cross-sectional area of the silver deposit toward light. This aggregation rationalizes the optical density loss observed with the increase in development time for the highly exposed areas of the film in formulations containing a large number of AgBr MCs.

The above observations suggest the following explanation. Initially, reduction of silver ion at the development centers, i.e., centers of selective thermolysis associated with the AgBr MCs, leads to formation of small particles of metallic silver and separation of stearate ion or stearic

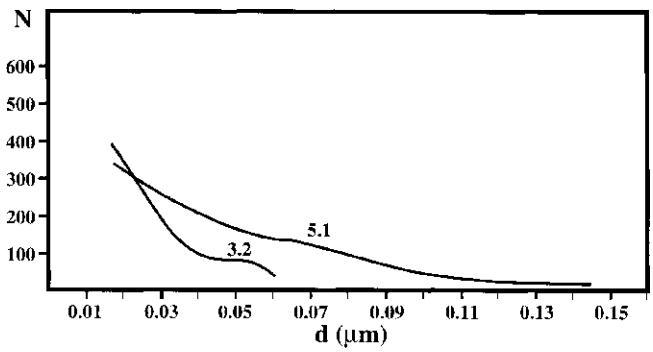

Figure 6. Distribution of AgBr MC diameters, d (μm), in TDPM samples 3.2 and 5.1.

acid. Silver stearate in combination with stearic acid, in the presence of solvent, is quite stable, and its colloidal particles are negatively charged.[9] We propose that the development centers, which have positively charged surfaces, attract these AgSt-containing spherical micelles. The melt of stearic acid, formed as a byproduct of the reduction reaction, provides a medium in which these particles can diffuse to the reaction site on the time scale of the development of the TDPM.

The morphology of the silver deposit in the unexposed but developed samples 2.4., 3.2. and 4.2. of Fig. 5 is quite different from that in the exposed samples. It is similar to that observable in the heated, unhalidized sample [Fig. 4(b)]. Much unreacted AgSt remains. Silver(0) particulates are much smaller in size than those in the exposed samples, generally ≤150 Å, and they are difficult to distinguish from the droplets that appear in unprocessed samples. Significantly they do not appear to be associated with the AgBr MCs, which remain clearly distinguishable in these TEM images. Accordingly fog formation may be nucleated either by spontaneous reduction of the AgSt-derived droplets or by thermolysis of AgSt itself. This latter process has been studied extensively by Andreev et al.[10]

Conclusions

We have carried out electrochemical, sensitometric, and electron microscope investigations of the reactions of the photosensitive phase of a thermally developable photomaterial. We found that formation of microcrystals of silver bromide by metathetical reaction of silver stearate with bromide in aqueous solution leads to precipitation of silver bromide as a separate phase, accompanied by dissolution of silver stearate microcrystals. The size of the AgBr microcrystals increases with increasing concentration of the brominating agent, but does not exceed 0.07 μm.

Latent image centers formed by the AgBr microcrystals are capable of catalyzing thermal development if the microcrystals have been formed in the presence of the carboxylate. The process of thermal amplification of the latent image centers may, however, be achieved on AgBr crystals having no physical contact with silver stearate. We propose that thermal development of latent image centers on AgBr crystals proceeds by diffusion of silver stearate-derived "droplets" to the development centers. Fog formation, on the other hand, nucleates independently of the AgBr microcrystals.

Acknowledgments. The authors wish to thank Prof. Lilia P. Burleva, Institute for Solid State Chemistry, Akademgorodok, Novosibirsk, Russia, and Dr. David R. Whitcomb and Dr. M. R. V. Sahyun, Dry Imaging Technology Center, 3M, for valuable assistance in preparing the English language version of this paper and for helpful comments. Statistical analyses, Eqs. 4 and 5, were provided by Dr. Sahyun. The authors also express gratitude to I. M. Gulkova and L. V. Sharova, who participated in many of the experiments reported here, and to 3M for underwriting the costs of publication of this work.

References

1. V. M. Andreev, E. P. Fokin, Yu. I. Mihaylov, and V. V. Boldyrev, *Zhur. Nauchn. i. Priklad. Fotogr. Kinematogr.* **24**: 311 (1979).
2. D. H. Klosterboer, in *Imaging Materials and Processes*, 8th ed., J. M. Sturge, V. Walworth, and A. Shepp, Eds., Van Nostrand Reinhold, New York, 1989, Chap. 9.
3. (a) J. Texter, in *IS&T's 48th Annual Conference*, IS&T, Springfield, VA, 1995, 186ff; D. S. Bailey, R. H. White, and J. Texter, US Patent 5,352,561 (1994); (b) H. Hirai and H. Naito, US Patent 4,604,345 (1987); T. Shibata, K. Sato, and Y. Aotsuka, in *Paper Summaries, 4th International Conference on Non-Impact Printing Technologies*, IS&T, Springfield, VA, 1988, pp. 362–365; E. Weyde, West German Patent 888,045 (1953).
4. J. W. Shepard, *J. Appl. Photogr. Eng.* **8**: 210 (1982).
5. D. A. Morgan, *Proc. SPIE* **1253**: 239 (1990).
6. W. J. Miller and R. W. Baxendale, US Patent 3,761,273 (1973).
7. Yu. E. Usanov, N. L. Kosobokova, and G. P. Tichomirov, *Opt. Mech. Ind.* (*Russ.*) **9**: 15 (1977); see also Ref. 8.
8. S. F. Cherenov, Yu. V. Fedorov, and V. N. Zakharov, *J. Inform. Rec. Mater.* **19**: 291 (1991); S. F. Cherenov, E. A. Galashin, and Yu. V. Fedorov, *ibid.* **18**: 107 (1990).
9. V. N. Zacharchenko, *Colloidal Chemistry*, Visshaya Shkola, Moscow, 1974, p. 147.
10. V. M. Andreev, L. P. Burleva, V. V. Boldyrev, and Yu. I. Mikhailov, *Izv. Sib. Otd. Akad. Nauk. SSSR, Ser. Khim. Nauk.* **4**(2): 58 (1983); V. M. Andreev, L. P. Burleva, and V. V. Boldyrev, *ibid.* **5**(5): 3 (1984); L. P. Burleva, V. M. Andreev, and V. V. Boldyrev, *J. Thermal Anal.* **33**: 735 (1988).